Electrodeposition of alloys from halide melts in solid state

Andrey Isakov [a], Aleksandr Chernyshev [a] [*], Alexey Apisarov [a], Yuri Zaikov [a]
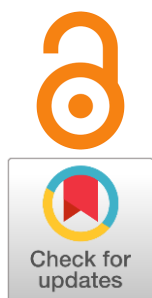
This review manuscript considers the conditions of metal co-deposition to obtain alloys in the solid state by electrolysis of halide molten salts. The conditions for co-deposition below the melting point of the deposited components from molten salts are considered. The possibilities of the method for co-deposition of alloys from molten salts under the action of direct electric current were summarized. The review considers the main factors affecting the co-deposition process in the solid state, including thermodynamic and kinetic aspects. Methods for the synthesis of various alloys system (melting point of which can be above 1000 °C) and experimental approaches used to organize the process of joint electrodeposition were considered. The results of a comparative analysis of experimental data obtained under various synthesis conditions were presented in order to determine the dependences between the electrolysis parameters and the composition of the alloys.

1. Introduction

Alloys and alloy coatings play a key role in engineering and industry. New materials offer a wide range of mechanical, chemical, and physical properties that can be used to the specific demands of the end application [1]. New methods of alloy production enable the development of materials with optimal combinations of strength, hardness, corrosion resistance, thermal conductivity, and other properties for various types of equipment and structures. Using of advanced materials contributes to increased efficiency and longevity of equipment, reduced maintenance and repair costs of structures, and ensures higher levels of safety and reliability in various industrial, engineering, and medical applications [2, 3].

New alloys and coatings can be used to improve the performance and service life of different devices and components [4]. The alloys can be used to increase the resistance of construction materials to wear, material fatigue, and other types of mechanical loads [5, 6]. New materials are especially relevant for applications in conditions of high temperatures, aggressive environments or corrosion, when standard materials cannot provide sufficient reliability.

Electrodeposition from molten salts is a promising method for the production of metals and alloys. Electrodeposition from molten salts, as a rule, has a relatively simple hardware design and does not require large expenses for the preparation of raw materials. Metals and alloys at temperatures below their melting point can be produced by electrodeposition from molten salts [7, 8].

The ability to obtain high-quality coatings with carefully controlled morphological, structural and functional characteristics is one of the key advantages of molten salt electrodeposition [9, 10]. The process of electrodeposition from molten salts can be controlled by the current density, temperature, and electrolyte composition. The use of various parameters of electrodeposition makes it possible to obtain materials

a: Institute of High Temperature Electrochemistry of the Ural Branch of the Russian Academy of Sciences, Ekaterinburg 620066, Russia

* Corresponding author: aac-vp@ihte.ru

with the required properties and regulate them by changing the composition and structure of the deposit in a certain range [11, 12].

Products with complex profile [13, 14] and composite materials [15, 16], including multilayer and functional coatings [17, 18], can be obtained by electrodeposition from molten salts. Electrolysis of molten salt is promising method to produced thin and uniform coatings with a high degree of adhesion to the substrate surface [19], as well as to precisely form three-dimensional structures and nanomaterials [20, 21]. Thus, molten salt electrodeposition is an effective tool for the production of a wide range of products and materials, including alloys, used in various industrial and technical fields, including electronics, aviation, medicine and energy.

Electrolysis of molten salts can be carried out at temperatures not exceeding 1000 °C in order to obtain alloys in the solid state. This temperature range is lower than the melting point of most elements used to produce the basis of high-temperature materials. For example, transition metals (except for Zn, Cd, Hg and Ag), beryllium, lanthanides (except for La, Ce, Pr, Eu, Yb) and silicon are solids up to 1000 °C.

Manuscripts devoted to the results of producing alloys in molten salts can be divided into several main areas:

– electrochemical co-deposition of several components from the melt;

– electrochemical deposition of one component from the melt onto a substrate capable of forming an alloy;

– current-free transfer of components from the melt to a substrate capable of forming an alloy.

The focus of this review is on the electrochemical co-deposition of multiple components from molten salts into a solid compact state. Analysis of the results of co-precipitation of elements from molten salts will allow summarizing existing approaches to obtaining functional coatings and drawing attention to possible stages for the development of practical technological processes.

2. Theoretical background

The rate and composition of electrochemical deposits from molten salts depend on thermodynamic and kinetic factors. Thermodynamics determines the possibility of co-deposition, while the kinetics of ion transport of melt components affects the rate of the process. A high deposition rate is required for practical application to ensure that protective coating deposition processes can be possible. The deposition rate depends on the diffusion coefficient of the ions contained in the melt.

Although the deposition rate is not a critical factor in the electrochemical synthesis of thin films and nanomaterials, it is still necessary to understand the conditions required for co-deposition. Changes in the deposition rate result in the composition, morphology, and properties of the materials.

Materials with various characteristics, such as film thickness, particle size, and crystal structure, can be obtained by electrolysis of molten salt at different deposition rates.

Although the deposition rate may not be the primary constraint, dependences of co-deposition conditions on material characteristics are crucial for the successful synthesis of thin films and nanomaterials via electrochemical methods.

Determining the conditions for the co-deposition of components from a melt is important to control the composition and properties of materials. The thermodynamic condition for the co-deposition of two components from a molten salt is based on the equality of electrode potentials. The thermodynamic condition for co-deposition of two components is [7]:

$$E_A^0 + \frac{RT}{n_A F} ln \frac{a_{Aox}}{a_{ARed}} = E_B^0 + \frac{RT}{n_B F} ln \frac{a_{Box}}{a_{BRed}}, \qquad (1)$$

where: E_A^0, E_B^0 – standard electrode potentials of components A and B, respectively, V; n_A, n_B – number of electrons for components A and B, respectively; a_{Aox}, a_{Box} – thermodynamic activity of components A and B in the melt; a_{ARed}, a_{BRed} – thermodynamic activity of components A and B in the alloy.

The value of the thermodynamic activity of the components in the reduced form (Equation 1) depends on the thermodynamics of the interaction of the alloy components. Thermodynamic activity for components that do not interact with each other (and are not soluble in each other) in the solid state:

$$a_{ARed} = a_{BRed} = 1. \qquad (2)$$

For components that can form ideal solid solutions:

$$a_{ARed} + a_{BRed} = 1. \qquad (3)$$

For components A and B that can form an A_xB_y intermetallic compound:

$$a_{ARed}^x \cdot a_{BRed}^y = \frac{1}{K_{eq.}}, \qquad (4)$$

where $K_{eq.}$ – reaction equilibrium constant of formation of an intermetallic compound A_xB_y.

Due to the absence of mass transfer in the solid phase, the concentrations of the alloy components depend on the intensity of the flows of the corresponding substances directed to the cathode.

Controlling the flow of ions to the cathode makes it possible to control the composition and properties of the deposited material:

$$I = I_A + I_B = \frac{z_A F D_A (C_0^A - C_S^A)}{\delta} + \frac{z_B F D_B (C_0^B - C_S^B)}{\delta}, \qquad (5)$$

where: I – electrolysis current, A; I_A, I_B – electrolysis current of component A and B, respectively, A; D_A, D_B – diffusion coefficients of ions A and B in the melt, cm$^2 \cdot$ s^{-1}; C_0^A, C_S^A – concentration of discharged ions A in the volume of the melt and near electrode surface, respectively, mol $\cdot$ cm^{-3}; C_0^B, C_S^B – concentration of discharged B ions in the volume of the melt and near the surface, respectively, mol $\cdot$ cm^{-3}; δ – diffusion layer thickness, cm; F – Faraday's constant equal to 96485.33 C $\cdot$ mol^{-1};

The relationship between the electrolysis current and the concentration of ions of precipitated substances in the melt can be established by Equation (5). The concentrations of components in the alloy are proportional to the flows of the corresponding ions to the cathode. Accordingly, the ratio of the concentrations of components in the alloy can be expressed through the equation of linear stationary diffusion:

$$\frac{C_A^{al}}{C_B^{al}} = \frac{z_A D_A (C_0^A - C_S^A)}{z_B D_B (C_0^B - C_S^B)}. \qquad (6)$$

Based on existing theoretical knowledge [7] about electrochemical co-deposition of metals from molten salts, it is possible to imagine the prospects for the practical implementation of this method. In work [7], academician A.N. Baraboshkin conventionally distinguishes two modes of deposition.

Thermodynamic (quasi-equilibrium) mode – the mode of deposition of components close to their standard potentials. In this mode, the deposition occurs in the range of current densities below the limiting diffusion for these components. The alloy composition slightly depends on the cathode current density of electrolysis under such conditions.

Kinetic mode – the mode of deposition of components at a difference in standard potentials of more than 0.2–0.25 V [7, 22]. The composition of alloy ceases to depend on the difference in standard potentials, and the concentration of the more electropositive component in the alloy decreases faster under such conditions.

Accordingly, we can conclude that the thermodynamic mode provides an opportunity for the implementation of alloys co-deposition processes of the required thickness. When implementing the kinetic mode, due to the large difference in electrode potentials, only cathode deposits of limited volume, gradient in composition, can probably be obtained. In this case, electrodeposition can be proceeded until the more electropositive component ends up in the melt.

Analysis of the theoretical background allows us to conclude that to maintain the required concentration of several components simultaneously in the molten salts during the electrodeposition of alloys is a complex scientific and technical task.

In practice, the implementation of both modes is probably only possible at the electrochemical reduction in a cell with an inert or gas-evaluating anode.

However, even if the electrode potentials of the deposited components are sufficiently close, maintaining their concentration in an electrochemical cell with inert or gas-evaluating anode de is a difficult task. Electrolysis in a refining-type cell with sacrificial anodes is complicated by contact exchange reactions between the more electropositive dissolved component of the melt and the more electronegative anode material.

In this case, during electrolysis in practice, an important role will be played by the choice of electrolysis temperature range and, as a consequence, the choice of the composition of the solvent melt.

3. Production of alloys by co-deposition from molten salts

The production data of alloys from molten salts should be summarized to analyze of the technical and technological possibilities of molten salt electrolysis. Identifying the similarities and differences obtained at different alloy electrodepositions will allow a deeper understanding of the application possibilities of alloy deposits in technological areas.

The number of fundamental studies on the co-deposition of metals from molten salts in the focus of our review is not large [23–34]. This can be explained by the fact that the unique properties of refractory and noble metals and the possibilities of the high-temperature electroplating method have been sufficient to meet the technical and technological needs of modern technology. Nevertheless, co-deposition of metals in molten salts offers opportunities to obtain materials and coatings with a new set of properties. The alloys production data by molten salt electrolysis were summarized in Table 1.

Table 1 – Preparation of alloys from molten salts.

#	Alloy	Melt, mol. %	ΔT, °C	Form metals in melt	Deposit	Note	Ref
1	Ir-Ru	NaCl-KCl-CsCl(eut.)	550–700	Chloride ion of Ir and Ru	coating, dendrite	i_k = 0.007–0.4 A · cm² , compact deposits were produced by electrolysis up to 0.05 A · cm²	[23, 24]
2	Ir-Rh	NaCl-KCl-CsCl(eut.)	not indicated	Chloride	coating, dendrite	Total concentration of Ir and Rh in the melt 2.5–4 wt. %	[25]
3	Ta-W	(60.4)LiF-(38.6)NaF-(1)K₂TaF₇	800	K₂TaF₇	coating	Content of W ions in the melt was 1–8 wt. %. Phases of Ta-7W, Ta-4W and Ta-1W were identified in deposits. Cathode material: low-carbon steel	[26, 27]
4	Ti-Nb	(42.25)NaCl-(42.25)KCl-(15.5)NaF	700	K₂TiF₆; K₂NbF₇	powder	Nb-Ti alloy powder (35.78 wt. %-Nb) by electrolysis of melt: NaCl-KCl-NaF (10.4 wt. %) K₂TiF₆ (10 wt. %)-K₂NbF₇ (1.4 wt. %)	[28]
5	Cr-Ni	(40)NaCl-(40)KCl-(20)NaF	800	Cr₂O₃, NiO	coating	i_k = 0.3 A/cm², cathode: low-carbon steel	[29]
6	Ta-Cr	(46.5)LiF-(11.5)NaF-(42)KF	750–800	K₂TaF₇, TaF₅, CrF₃, CrO₂	coating	i_k = 0.008–0.050 A/cm², at TaF₅ 10 wt. %/K₃CrF₆-Ta-rich tantalum-chromium alloys at CrF₃ 6 wt. %/TaF₅ 0.05 wt. %-Cr-rich chromium-tantalum alloys	[30]
7	Al-Pt	(61)AlCl₃-(26)NaCl-(13)KCl	175	PtCl₂	coating	Phases of Pt, AlPt₂, AlPt₃, were identified in deposits produced by potentiostatic electrolysis (culonostatic 40 C · cm⁻²)	[31]
8	Al-Ta	(61)AlCl₃-(26)NaCl-(13)KCl	150	TaCl₅	coating	Concentration of Ta ions in molten salt was 20 mM. Potentiostatic electrolysis *vs* Al/Al(III): −0.05 V (Al₉₆Ta₄), −0.02 V (Al₇₃Ta₂₇), and (c) 0.1 V (Al₂₈Ta₇₂). potentiostatic electrolysis (culonostatic 30 C · cm⁻²), cupper substrate, concentration 7 · 10⁻² mol. · dm⁻³	[32]
9	Al-Cr-Ni	(61)AlCl₃-(26)NaCl-(13)KCl	150	CrCl₂; NiCl₂	coating	Glassy carbon substrate The saturated concentration of CrCl₂ and NiCl₂ dissolved in the molten salt was found to be about 8 · 10⁻² and 5 · 10⁻² mol. · dm⁻³ potentiostatic electrolysis (culonostatic 40 C · cm⁻²)	[33]
10	Ti-V	LiCl-KCl(eut.)	427	VCl₃, TiCl₂	dendrites	Potentiostatic electrolysis, 0.45 mol. % TiCl₂-0.34 mol. % VCl₃ (Ti-60 V) 0.09 mol. % VCl₃-0.46 mol. % TiCl₂ (Ti-11 V)	[34]

The electrochemical co-deposition of Ir-Ru from NaCl-KCl-CsCl containing $C_{Ir^{3+}}$ 0.8 mol. % and $C_{Ru^{3+}}$ 0.95 mol. % was investigated. Stationary potentials of Ir and Ru were measured at 500–700 °C in eutectic melts of NaCl-KCl-CsCl containing a mixture of Ir and Ru chlorides. Stationary potentials of Ir and Ru were more positive than their equilibrium values due to alloying in the surface layer by metal [23]. During the electrodeposition of compact layers of Ir-Ru alloys at low current densities, preferential deposition of the more electronegative Ru into the alloy was observed. Depolarization was observed at the cathodic deposition of alloys. Ir-Ru alloys (solid solutions) were deposited by electrolysis at current densities up to the limiting diffusion current. A powdery dendritic mixture of separate Ir and Ru crystals were electrodeposited at higher current densities than the limiting diffusion current.

The exposure of Ir and Ru electrodes in a NaCl-KCl-CsCl(eut.) melt containing Ir^{3+} and Ru^{3+} ions in an open circuit was studied. Chemical interactions (7)–(10) were identified based on the results of the data analysis [22].

Cementation reaction:

$$Ir^{3+} + 2Ru = (Ir\text{-}Ru) + Ru^{3+}, \qquad (7)$$

Contact exchange reaction:

$$Ru^{3+} + 2Ir = (Ir\text{-}Ru) + Ir^{3+}, \qquad (8)$$
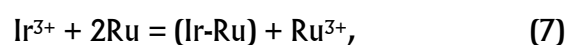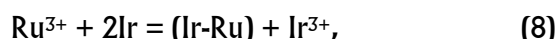
Alloy production by disproportionation reactions:

$$4Ru^{3+} + Ir = (Ir\text{-}Ru) + 3Ru^{4+}, \qquad (9)$$

$$4Ir^{3+} + Ru = (Ir\text{-}Ru) + 3Ir^{4+}. \qquad (10)$$
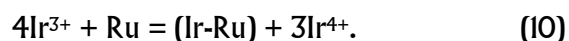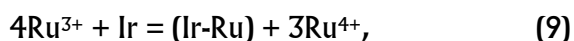
Cementation, contact exchange, and disproportionation reactions are the main mechanisms of the chemical processes that accompany electrochemical deposition [22]. The possibility of reactions of type (7)–(10) must be taken into account to control the composition and properties of alloys. In this case, the possibility of reactions strongly depends on the nature of the co-deposited substances. Understanding these mechanisms is of great importance, along with the electrode electrocrystallization of individual components, to optimize the processes of obtaining alloys in molten salts.

Reactions (8)–(10) significantly affect the process of obtaining alloys by currentless deposition in the electrochemical cell. Reaction (7) has a significant impact and will be present under any conditions, except for $\Delta G = 0$ at thermodynamic equilibrium. Co-deposition of two noble elements is an excellent model experiment that has allowed identification of the chemical processes accompanying the electrochemical reduction process.

Continuous coatings can be produced by electrodeposition of two components from molten salt [2]. The dependence of the composition of Ir-Ru alloys on the cathodic current density and the electrolyte composition $(CsCl\text{-}NaCl\text{-}KCl)_{eut}$-$IrCl_3$-$RuCl_3$ was determined [24]. The structure and composition of the Ir-Ru alloys as a function of electrolysis conditions were studied. It was found that the maximum temperature at which continuous layers of Ir-Ru can be obtained is higher than that of pure Ir or Ru. Continuous layers were deposited as solid solutions over the entire range of compositions (from 0 to 100 % of each component). Preferential deposition of the more negative component (ruthenium) into the alloy was observed. The composition of Ir-Ru alloys as a function of the deposition conditions is presented in Figure 1. Several types of alloy structure were identified: columnar, spherulitic, layered, and spiral. The conditions leading to the deposition of layered structures were analyzed.
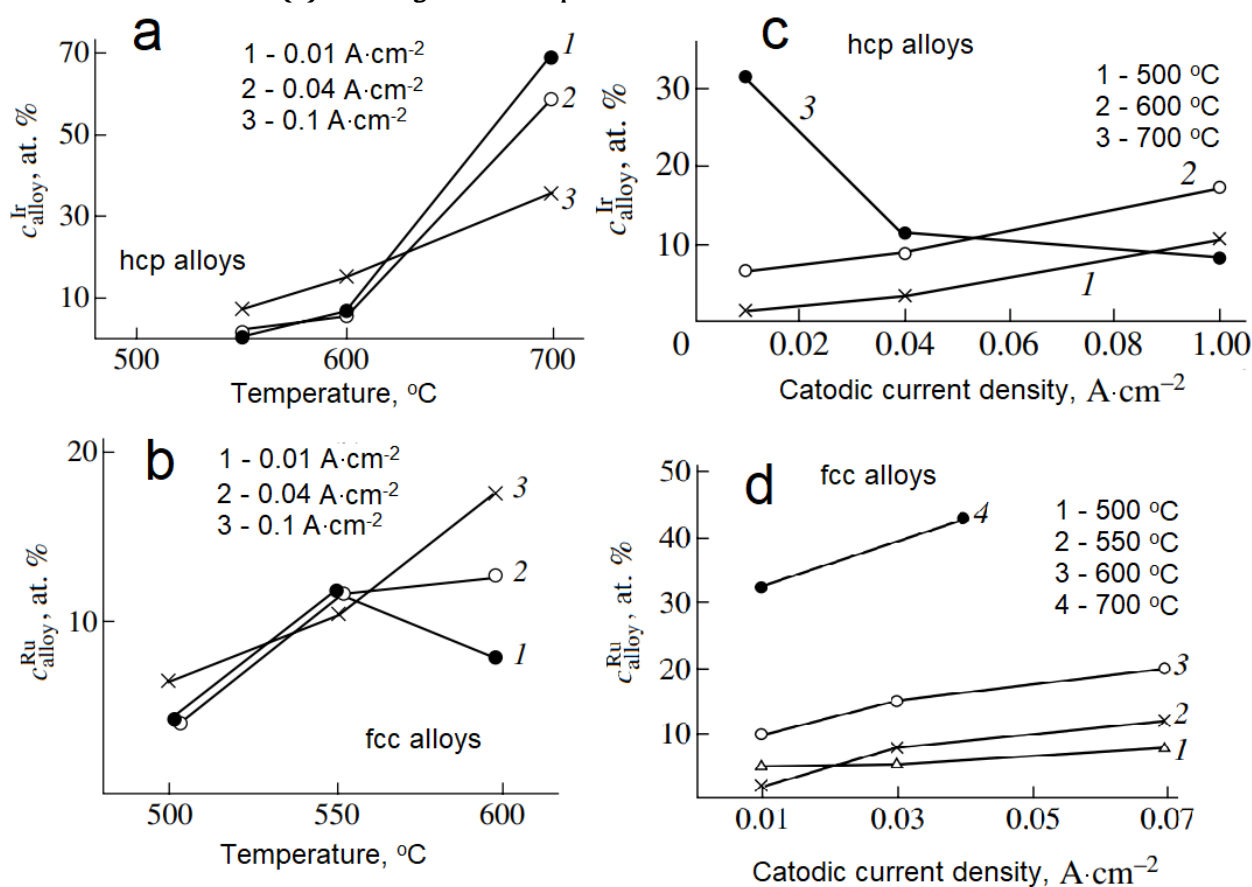

Figure 1 The dependences of compositions of Ir-Ru alloys: (a, c) – hcp alloys (melt contains 4.3 wt. % Ir and 2 wt. % Ru); (b, d) – fcc alloys (melt contains 3.4 wt. % Ir and 0.5 wt. % Ru) [22–23].

The study of the phase composition of the deposits (Figure 1) showed that the crystallization of the alloys in terms of chemical composition was consistent with the Ir-Ru phase diagram [35]. In the work [25], the technical feasibility of using Ir-based alloys (Ir-Rh) produced by electrolysis of a melt (CsCl-NaCl-KCl)$_{eut}$ containing iridium and rhodium ions was demonstrated. Electrochemical Ir-Rh alloys were used for liquid-propellant thruster production.

In works [26, 27], the possibility of electrochemical deposition Ta-W alloys from LiF-NaF-K$_2$TaF$_7$ melt was studied. Deposition was carried out by a method called MARC (Multi-Anode Reactive Alloy Coating). The MARC method uses an electrochemical cell design that provides for the use of 2 anodes (Ta and W). Ta and W anodes were used to maintain the concentration of the Ta and W ions in the melt during electrolysis. Two modifications of the MARC method (MARC 1 and MARC 2) were developed (Figure 2).

Both MARC methods have advantages that can be used for electrodeposition of solid-state alloys by electrolysis of molten salt.

MARC 1 provides the ability to obtain gradient coatings on the cathode surface.

The MARC 2 method provides the possibility of alloy coatings production with a specific ratio.

The MARC 2 method had allowed changing the composition of the deposit due to the distribution of current lines in the electrochemical cell. Increasing the distance between the anodes of different metals and the cathode had also allowed influencing the composition of the cathodic deposit by changing the resistance of the melt layer and the length of the ion path from the anode to the cathode.
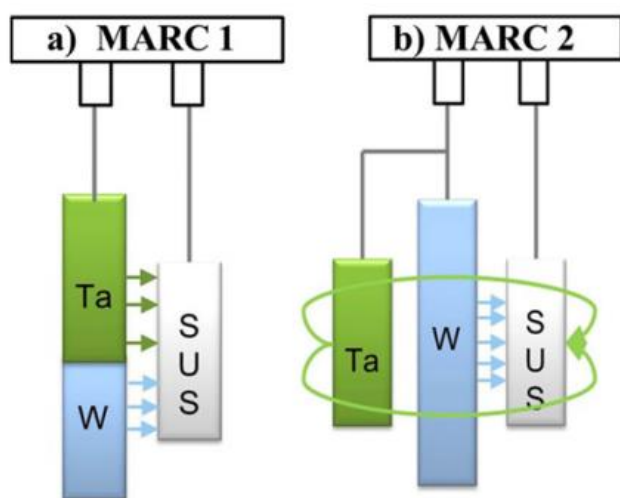

Figure 2 Design of MARC methods [4].

Ta-W coatings [26] were obtained by electrolysis of melts on a SUS316 substrate using the MARC method. The coatings were found to consist of a Ta-W solid solution with a tantalum-rich phase and a single-phase tungsten. The Ta-W alloy deposit in the initial coated film had smaller grains (probably due to the more suitable nucleation sites at the SUS316L substrate interface), which are the dominant parameters. The hardness of the pure tantalum coating film was 153.7 Hv, so the increase in hardness resulting from the concentration of tungsten, ranging from 5.98 % (165.2 Hv) to 12.9 % (244.5 Hv), will contribute to its use in a wide variety of harsh engineering process environments.

Co-deposition of Ti-Nb alloys was investigated [28]. Niobium–titanium alloys can be prepared by co-deposition in NaCl-KCl-NaF melts. The electrochemical behavior of niobium and titanium was investigated first separately, then together, using the following methods: linear sweep voltammetry, semi-integration and semi-differentiation of cyclic voltammograms, and square-wave voltammetry. The reduction processes of niobium (V) and titanium (IV) are, respectively, Nb(V) → Nb(IV) → Nb and Ti(IV) → Ti(III) → Ti. Each of the first steps proceeds in the same potential range, whereas niobium metal is obtained at a more positive potential than titanium.

In the case of mixtures of Ti and Nb ions in the melt, the electrochemical curves derive from the addition of each separated system and show three peaks (Nb(V) → Nb(IV) and Ti(IV) → Ti(III); Nb(IV) → Nb; Ti(III) → Ti) in the cathodic sense. Co-deposition of Nb-Ti alloys was prepared by galvanostatic electrolysis and further analyzed with a microprobe.

The Nb-Ti alloys can be obtained by electrolysis of NaCl-KCl-NaF-K$_2$TiF$_6$-K$_2$NbF$_7$ at an electrode potential more negative than the potential of Ti deposition. The alloy composition depends on the Nb content in the melt, since Nb is a more electropositive metal. Thus, Nb was deposited by electrolysis at the limiting current. It was hypothesized that, since the Nb current is limiting, the total current will mainly determine the Ti content. That is, increase of the current density leads to increase in the titanium concentration in the cathodic deposit.

In work [29] Cr-Ni alloy/low-carbon steel surface composites were prepared by molten salt co-deposition in NaCl, KCl, NaF, Cr$_2$O$_3$, and NiO melt salt system at 1073 K. The kinetics of the Cr-Ni alloy electrodeposition was studied.

A gradient layer of Cr-Ni alloy was formed on the surface of low-carbon steel. The Cr-Ni alloys were produced by electrochemical reduction and high-

Table 2 – Conditions of Ta-Cr coatings electrodeposition Ta-Cr coatings from FLiNaK melt [30].

#	Solute 1 TaF_5 [a], wt. %	Solute 2 CrF_3 [b], wt. %	T, °C	Current density, mA · cm⁻²	Current efficiency, %	Deposition rate, μm · h⁻¹	Coating
1	10		755	17.5	99.3	13	Ta
2	10		755	27.7	99.6	23	Ta
3	10	0.5	800	18.7	92.2	14	Ta-(2.2 wt. %) Cr
4	10	1.0	800	36.1	89.4	23	Ta-(4.7 wt. %) Cr
5	10	1.0	800	29.1	88.2	20	Ta-(4.7 wt. %) Cr
6	10	1.5	800	20.4	74.4	13	Ta-(6.6 wt. %) Cr
7	10	0.5–1.5	750–800	5–40	–	–	Ta-rich alloys
8	0.05	6	800–835	0.8–50	–	–	Cr-rich alloys

[a] – as K_2TaF_7; [b] – as K_3CrF_6.

temperature solid diffusion through a combination of chromium and nickel ions mass transfer in the molten salt. Chromium and nickel ions were simultaneously reduced on the cathode surface through two and one steps, respectively. The diffusion coefficients of chromium and nickel atoms in the surface composite were calculated to be $1.16 \cdot 10^{-14}$ m² · s⁻¹ and $1.44 \cdot 10^{-14}$ m² · s⁻¹ according to the detection data of the deposition layer. The concentration of ions in the electric double layer near the cathode cannot be rapidly supplemented due to the low mass transfer rate. The low mass transfer rate limits the speed of the entire preparation process. The results show that chromium and nickel ions were simultaneously reduced on the cathode surface through two and one steps, respectively. The alloy layer (Fe content of 64.52 wt. %, Ni content of 28.96 wt. %, and Cr content of 6.52 wt. %) was deposited on the surface of a low-carbon steel substrate.

In work [30] electrodeposition of Ta-Cr coatings from FLiNaK was investigated. The conditions of electrodeposition of Ta-Cr coatings are presented in Table 2. Ta-Cr coatings were electrodeposited as a continuous layer of alloy. In fluoride melts, Ta and Cr considered in [30] are characterized by oxidation states when dissolved in the melt: Ta^{5+} [36], Cr^{3+} [37]. The results of work [9] are consistent with the conclusions that can be drawn based on Equation (6). The data from [8] illustrate that the ratio of the fluxes of the deposited ions is proportional to the ratio of the concentrations of these ions in the electrode deposit.

Data from [9] make it possible to plot the dependence of the concentration ratio in the sediment on the concentration ratio in the electrolyte (Figure 3).

The dependence presented in Figure 3 [30] is consistent with Equation (6). The slope of the approximating line (Figure 3) obviously depends significantly on the difference in concentrations in the bulk and near-electrode region. Developing a process for


y = 2.2229x - 0.6561
R² = 0.9975
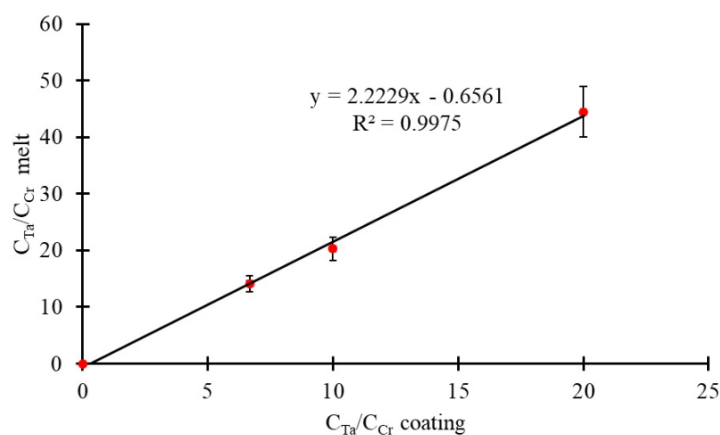
Figure 3 Experimental dependence of the ratio of tantalum and chromium concentrations in the electrode deposit and in the electrolyte.

alloy electrodeposition with a specific concentration ratio of components will require constructing experimental dependences similar to that shown in Figure 3. In the deposition of alloys, as shown in [23, 24], cementation and contact exchange reactions could occur. The rate of cementation and contact exchange reactions significantly depends on the process temperature. In [3–34], it was proposed to use low-temperature melts based on the NaCl-KCl-AlCl₃ system for alloys electrodeposition. NaCl-KCl-AlCl₃ melts are characterized by very low melting temperatures. However, experimental work with NaCl-KCl-AlCl₃ melts is extremely complicated due to their hygroscopicity. Reproducible data in [31–33] indicate careful preparation and high experimental technique. As can be seen from the results, the low temperature of the experiments [31–33] significantly reduced the influence of cementation and contact exchange reactions on the final result of electrodeposition.

In work [31], the electrodeposition of Al-Pt alloys using potentiostatic electrolysis in a molten AlCl₃-NaCl-KCl containing PtCl₂ was investigated. To form Al-Pt

alloys with high melting points, molten salt electrolysis was attempted using AlCl$_3$-NaCl-KCl molten salt containing PtCl$_2$ at 448 K. The voltammogram showed cathodic reduction of Pt ions to start at a potential of 1.4 V *vs* Al/Al(III) in the molten salt. The deposition of pure Pt was possible at 1.2 V, and there was co-deposition of Al and Pt at potentials more negative than 1.0 V. The co-deposit was a mixture of intermetallic compounds of AlPt$_2$ or AlPt$_3$. The ratio of the Pt in the electrodeposits decreased with increasingly negative potentials from 100 at. % at 1.2 V to 25 at. % at 0.0 V.

In work [32] electrodeposition of Al-Ta alloys in NaCl-KCl-AlCl$_3$ molten salt containing TaCl$_5$ was investigated. Al-Ta alloys were electrodeposited by electrolysis of AlCl$_3$-NaCl-KCl melt containing TaCl$_5$ at 423 K. The voltammogram showed two cathodic waves at 0.45 V and 0.7 V *vs* Al/Al(III), which may correspond to reduction from Ta(V) to Ta(III) and from Ta(III) to tantalum metal, respectively. Electrodeposits of Al and Ta were obtained in the range from −0.05 to 0.3 V and the highest concentration of Ta in the electrodeposit was 72 at. % at 0.3 V. With increasing Ta concentration in the alloy, the morphology of the electrodeposits became powdery and the particle size smaller.

In work [33] co-deposition of elements for production of Al-Cr-Ni alloys, using constant potential and potential pulse techniques in AlCl$_3$-NaCl-KCl molten salt were studied. To improve the oxidation resistance of TiAl intermetallic compound under high temperature condition, cathodic co-deposition of Al-Cr and Al-Ni alloy was carried out by constant potential control or potential pulse control in AlCl$_3$-NaCl-KCl molten salt containing CrCl$_2$ and/or NiCl$_2$ at 423 K. Cathodic reduction of Ni and Cr starts at potential of 0.8 and 0.15 V versus Al/Al^{3+} in the molten salt, respectively. The co-deposition of Al, Cr, and Ni occurred at potentials more negative than −0.1 V to form a mixture of intermetallic compounds of Cr$_2$Al, Ni$_3$Al, and Al$_3$Ni. The concentration of Cr in the deposit increased to 43 at. % at −0.1 V; however, the Ni concentration in the deposit was 6 at. % at the same potential. The concentration of Ni and Cr further decreased with more negative potential to 1 at. % at −0.4 V. The potential pulse technique enhanced the Ni concentration in the deposit to about 30 at. %, due to anodic dissolution of Al content from the deposit at the higher side of potential on the potential pulse electrolysis. For preparation of an oxidation resistance layer under high temperature condition, co-deposition of intermetallic compounds of Cr$_2$Al, Ni$_3$Al, and Al$_3$Ni as well as metallic Al was done by potentiostatic electrolysis in 61 mol. % AlCl$_3$-26 mol. % NaCl-13 mol. % KCl containing CrCl$_2$ and NiCl$_2$ at 423 K.

In works [31–33] it was shown that the dissolution of platinum, tantalum, nickel, and chromium chloride compounds in molten AlCl$_3$-NaCl-KCl occurs at approximately the same rate, and after 1 hour, the melts become saturated with potential-determining elements.

In work [34] co-deposition of Ti and V from a eutectic LiCl-KCl electrolyte contained of VCl$_3$ and TiCl$_2$ at 700 K was investigated. While the addition of metallic titanium to the electrolyte caused vanadium depletion by a displacement reaction, metallic vanadium addition created and stabilized divalent vanadium ions in the melt, which are supposed to positively affect the deposition process. Electrochemical experiments were carried out using different electrolyte concentrations [34], in which the correlation between applied potential, electrolyte concentration, and composition of the deposit was established. The composition and morphology of the obtained deposits were strongly affected by the electrolysis conditions. Electrodeposited vanadium-rich Ti-V alloys were found to grow as dendrites, whereas the titanium-rich alloys exhibited a dense cauliflower-like surface morphology. In contrast to deposits of the single elements, which are composed of comparably large, faceted crystals, the Ti-V alloys obtained in this study were very fine grained, especially those with vanadium contents around 10–15 at. %. Transmission electron microscopy revealed that, depending on the composition of the deposit, either a biphasic $\alpha + \beta$ microstructure in the case of low vanadium contents or β-(V, Ti) with small amounts of ω phase for high vanadium contents were found.

The available data on alloys production by co-deposition from molten salts allow the development of alloy production technologies in several directions:

- electrodeposition of alloys from melts with feeding of the electrolytic cell by chemical compounds;

- electrodeposition of alloys from molten salts in cells with soluble metal anodes at close standard potentials conditions;

- electrodeposition of alloys from molten salts with a large difference in conditional standard potentials in low-temperature melts under conditions of cementation and contact exchange reactions with low rate.

4. Structure and morphological structure of cathode alloys produced by electrodeposition of from molten salts

The structure and morphology of the alloys play a crucial role in determining their final application. The

structure of an alloy can be characterized by the arrangement and size of the various phases and components, while the morphology describes the shape and size of these phases. These characteristics influence the mechanical, electrical, and chemical properties of the alloy [39–42]. For instance, alloys with a fine-grained structure and smooth morphology exhibit higher strength and wear resistance. This makes them suitable in components subjected to high loads and friction. On the other hand, alloys with a dendritic structure tend to have a higher surface area. This makes them suitable as catalysts. Therefore, understanding and controlling the structure and morphology of alloys is crucial to developing materials that meet specific performance requirements [43].

The absence of oxygen impurities in the electrolysis of molten salts has a significant influence on the structure of electrodeposited coatings. Oxygen, being a strong oxidant, can react with metals, forming oxides and other compounds, which leads to a change in the physicochemical properties of the deposits. In the absence of oxygen, these reactions are suppressed, which allows the production of cleaner and more homogeneous coatings.

Electrodeposited coatings manufactured in the absence of oxygen can be characterized by their higher coating density [43]. Metal atoms have the opportunity to form a more perfect crystal lattice, which leads to improved mechanical and electrical properties of the deposits. In addition, oxygen in the melt causes the appearance of defects (microcracks, micropores) in the electrolytic deposit.

The absence of oxygen affects the morphology on electrodeposited coatings. Deposits obtained under low oxygen conditions yield a smoother and more homogeneous surface due to even crystal growth, without the formation of dendrites or other undesirable structures which can be experienced in the presence of oxygen. Improved morphology contributes to better adhesion to the substrate and higher performance characteristics.

The electrodeposition of compact deposits is of greatest interest for the production of products using high-temperature electroplating in molten salts [44–47].

The regularities of obtaining continuous layers of cathodic deposits allow for the development of technological processes for the production of products and protective coatings.

Figure 4 shows photographs of cross-sections of continuous alloy deposits obtained by electrolytic deposition in molten salts. The structure and morphology of the continuous deposits (Figure 4) of the alloys are typical for the electrolytic deposits of individual metals obtained from molten salts. In the example of noble metal alloys, it can be seen that the deposits have a columnar structure (Figures 4a and 4b). Overall, there is a range of conditions under which continuous coatings can be obtained. That is confirmed by data of works [23, 25–27, 30, 32, 34].

When alloys are used, it is important to understand whether the alloys are chemically and phase-homogeneous. In work [24], it was shown that the composition of the Ta-Cr alloy with a total content of 6.6 at. % Cr can vary along the cross-section The available literature regarding the phase composition of the deposited alloy layer is contradictory [22, 26, 32]. The phase composition patterns of electrolytic deposits had to be investigated for each new alloy produced by electrolysis of molten salts. The results of works [22, 26, 32] suggested that phase composition could be predicted by focusing on the ratio of component concentrations in the melt, provided that there was an experimental relationship between the concentration ratios (Figure 3). In this case, the phase composition could be predicted using phase diagrams of alloy elements. For instance, the Ta-W phase diagram [37] indicated that the components had unlimited solubility in each other. The Ta-W phase diagram [37] has been in agreement with the XRD data (Figure 5 [26]).

Electrolysis of molten salts is a promising method for producing coatings and products from various alloys. The electrolytic process allows control over the composition and structure of deposits, creating materials with unique properties. It is necessary to know the conditions of electrolysis, including current density, temperature, and electrolyte composition to obtain continuous deposits that met the requirements of practical application.
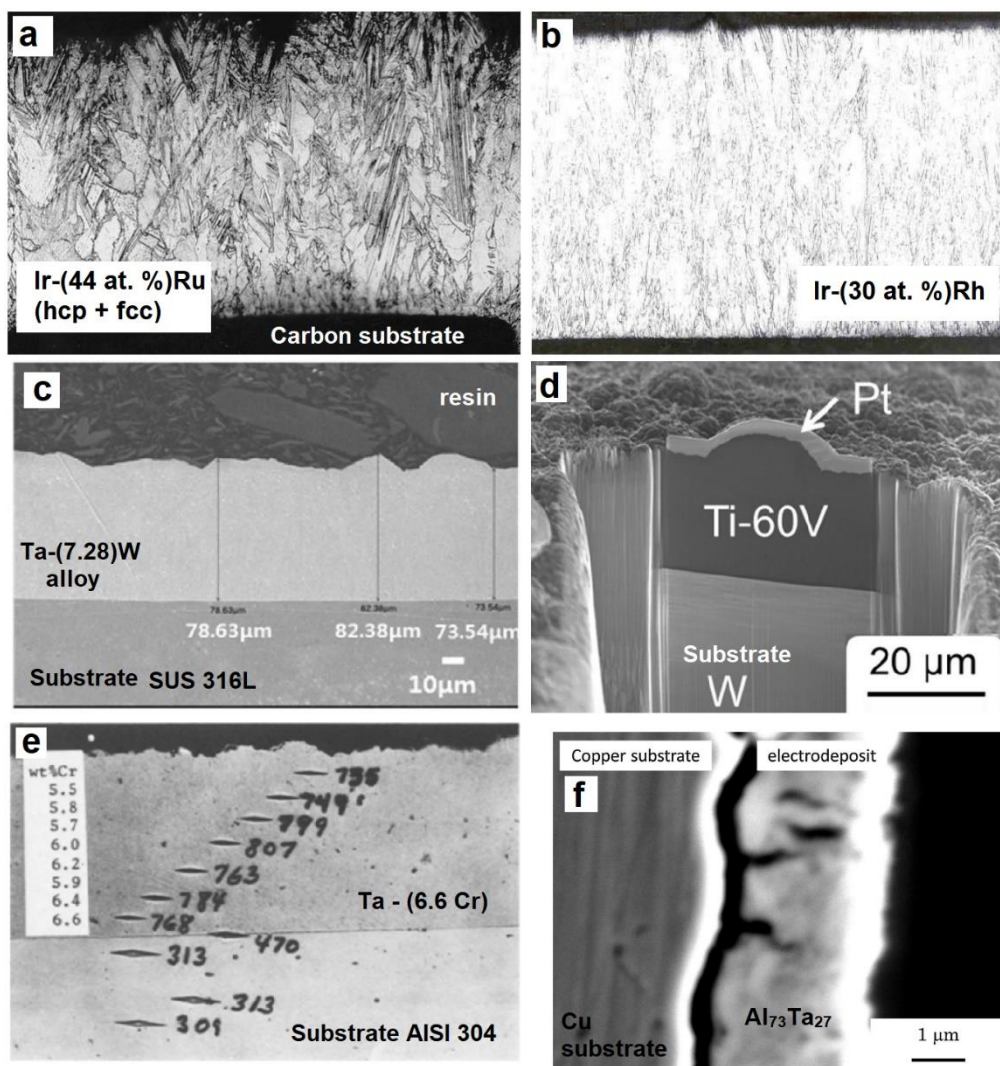
Figure 4 Cross-section observation of alloy electrolytic deposits produced by electrolysis of molten salt: (a) – [23]; (b) – [25]; (c) – [26, 27]; (d) – [34]; (e) – [30]; (f) – [32].
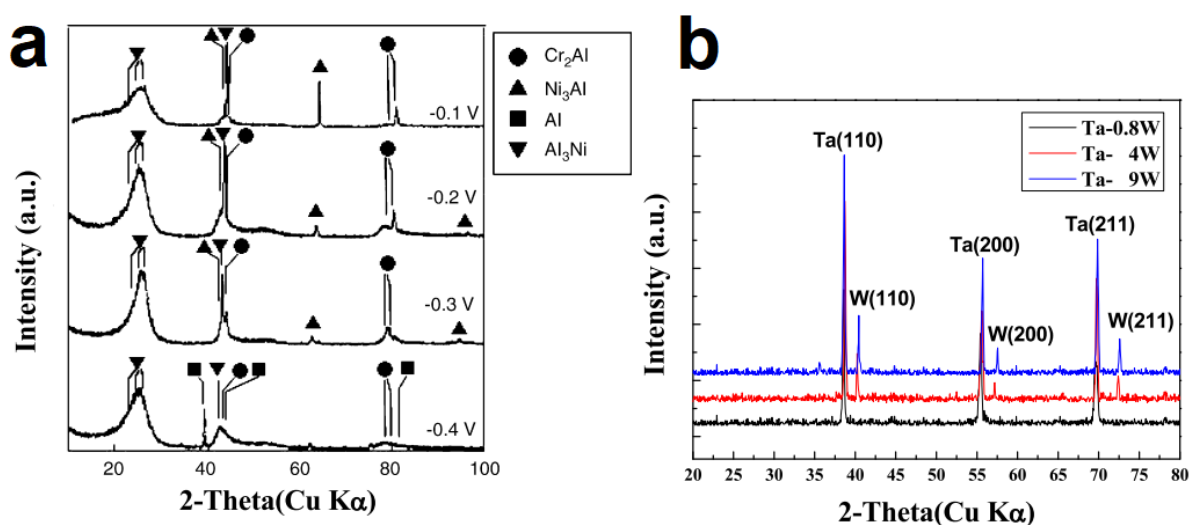

Figure 5 XRD patterns of alloys produced by electrolysis: (a) – Al-Cr-Ni alloys prepared in AlCl$_3$-NaCl-KCl at 150 °C [33]; (b) – Ta-W alloy coatings prepared in LiF-NaF melts containing 1 mol. % K$_2$TaF$_7$ at different W contents at 800 °C [26].

5. Conclusions

Upon reviewing the available literature on the production of functional coatings, and their alloys using high temperature electrochemical reactors, it can be demonstrated the feasibility of the technology. Electrolysis performed in molten salt systems can be achieved at temperatures lower than the melting point of their respective components. A key technological characteristic of the process of producing alloys is the dependence of the ratio of alloy components in the electrolytic deposit and melt, tied to the electrolysis conditions. Prediction of the phase composition can be carried out in accordance with phase diagrams of co-precipitated elements at the temperature of the deposition process. Preparation of alloys by electrolysis of melts at close values (with a difference of less than 0.25 V) of equilibrium potentials using soluble anodes. The production of alloys with a greater difference in the equilibrium potentials of the components is possible under conditions of low temperatures, when carburization and contact exchange reactions occur at a low rate.

In the process of solid deposit electrodeposition that meets the requirements of practical applications, it is necessary to take into account the electrolysis conditions, including current density, temperature, and composition of the electrolyte.

During the electrolysis of molten salts, various electrochemical reactions can occur, leading to the formation of multiphase structures. Therefore, particular attention should be paid to the patterns of changes in the phase and chemical composition along the length of the cross-section of the material. Experimental data can enable the development of technological electrolysis regimes that ensure the production of alloy deposits with specified properties and a uniform chemical composition throughout the entire thickness of the material.

The study of co-deposition of an alloy from molten salts is accompanied by significant difficulties due to the complexity of the experimental conditions and the lack of fundamental knowledge in this area. Despite significant progress in the electrodeposition of metals from molten salts, a wide range of issues related to the co-deposition of alloys still remains unexplored. The unreliable nature of the data prevents the full potential of co-deposition of metals and non-metals from molten salts from being fully realized. Limited understanding of the fundamental deposition mechanisms that influence the alloy production process makes it difficult to optimize the parameters and predict the properties of the alloys. Electrodeposition of alloys with more than 3 components is an unexplored area.

Understanding the factors influencing the morphology, composition, and properties of sediments will allow us to develop this process and use it to produce new materials with improved characteristics.

Supplementary materials

No supplementary materials are available.

Funding

Acknowledgments

Author contributions

We follow the widely recognized CRediT taxonomy (https://credit.niso.org) to highlight a unique role of each co-author. Please indicate full name(s) of the responsible author(s) for the following contributor roles after the colons:

Isakov Andrey: Conceptualization; Data curation; Formal Analysis; Writing – Original draft.

Chernyshev Aleksandr: Writing – Review & Editing; Data curation; Methodology; Project administration; Supervision. Writing – Original draft.

Apisarov Alexey: Writing – Review & Editing; Writing – Original draft.

Zaikov Yuri: Funding acquisition.

Conflict of interest

The authors declare no conflict of interest.

Additional information

Andrey Isakov, Scopus Author ID: 54684064200, Orcid: 0000-0002-0192-3048;

Aleksandr Chernyshev, Scopus Author ID: 57214986102, Orcid: 0000-0002-5700-4219;

Alexey Apisarov, Scopus Author ID: 14021004000, Orcid: 0009-0007-0730-9405;

Yuri Zaikov, Scopus Author ID: 6603601069, Orcid: 0000-0001-6138-3955.

References

1. Moschetti M, Perrière L, Couzinié J-P, Kruzic JJ, Gludovatz B, A Novel Strategy for the Design of Compositionally Complex Alloys for Advanced Nuclear Applications, Appl. Mater. Today, **38** (2024) 102164. https://doi.org/10.1016/j.apmt.2024.102164

2. Mullin KM, Martin JH, Roper CS, Levi CG, Pollock TM, Transpiration Cooling of a Porous Nb-Based Alloy in High Heat Flux Conditions, International Journal of Thermal Sciences, **196** (2024) 108758. https://doi.org/10.1016/j.ijthermalsci.2023.108758

3. Wood RJK, Lu P, Coatings and Surface Modification of Alloys for Tribo-Corrosion Applications, Coatings, **14(1)** (2024) 99. https://doi.org/10.3390/coatings14010099

4. Singh Tanwar R, Jhavar S, Ti Based Alloys for Aerospace and Biomedical Applications Fabricated through Wire + Arc Additive Manufacturing (WAAM), Mater. Today Proc., **98** (2024) 226–232. https://doi.org/10.1016/j.matpr.2023.11.121

5. Das A, Majumdar S, Insights into a Novel Refractory Multi Principal Element Alloy $(Mo_{98}W_2)_{85}Nb_{10}(TiHf)_5$ and Advancements in Oxidation Resistance upto 1300 °C through Silicide Coatings, Scr. Mater., **245** (2024) 116063. https://doi.org/10.1016/j.scriptamat.2024.116063

6. Wen Y, Zhao Y, Zhang Z, Wu Y, et al., Electrodeposition of Ni-Mo Alloys and Composite Coatings: A Review and Future Directions, J. Manuf. Processes, **119** (2024) 929–951. https://doi.org/10.1016/j.jmapro.2024.03.099

7. Baraboshkin AN. Elektrokristallizatsiya metallov iz rasplavlennykh soley [Electrocrystallization of Metals from Molten Salts]. Moscow: Nauka; 1976. 99–106 pp. Russian.

8. Gu Y, Liu J, Qu S, Deng Y, et al., Electrodeposition of Alloys and Compounds from High-Temperature Molten Salts, J. Alloys Compd., **690** (2017) 228–238, https://doi.org/10.1016/j.jallcom.2016.08.104

9. Zhu L, Wang J, Wang Z, Ye Y, et al., Morphologies and Textures of Rhenium Coatings Electrodeposited in Chloride Molten Salts, Surf. Coat. Technol., **428** (2021) 127887. https://doi.org/10.1016/j.surfcoat.2021.127887

10. Yuan W, Zhu L, Zhang H, Feng S, et al., Surface Morphology, Microstructure and Emissivity of Rhenium Electrodeposited from Molten Salts, Surf. Coat. Technol., **474** (2023) 130122. https://doi.org/10.1016/j.surfcoat.2023.130122

11. Qi Y, Tang Y, Wang B, Zhang M, et al., Characteristics of Tungsten Coatings Deposited by Molten Salt Electro-Deposition and Thermal Fatigue Properties of Electrodeposited Tungsten Coatings, Int. J. Refract. Metals Hard Mater., **81** (2019) 183–188. https://doi.org/10.1016/j.ijrmhm.2019.03.006

12. Laptev M, Khudorozhkova A, Isakov A, Grishenkova O, et al., Electrodeposition of Aluminum-Doped Thin Silicon Films from a $KF-KCl-KI-K_2SiF_6-AlF_3$ Melt, Journal of the Serbian Chemical Society, **86** (2021) 1075–1087. https://doi.org/10.2298/JSC200917065L

13. McKechnie T, Hasanof T, Shchetkovskiy A, Zaluki M, et al. Green Monopropellant 100mN Thruster. In: Proceedings of the AIAA Propulsion and Energy 2021 Forum; 2021 August 9–11; American Institute of Aeronautics and Astronautics: Reston, Virginia. https://doi.org/10.2514/6.2021-3591

14. Anflo K, Mollerberg R, Neff K, King P. High Performance Green Propellant for Satellite Applications. In: Proceedings of the 45th AIAA/ASME/SAE/ASEE Joint Propulsion Conference & Exhibit; 2009 August 2–5; American Institute of Aeronautics and Astronautics: Denver, Colorado. https://doi.org/10.2514/6.2009-4878

15. Isakov AV, Nikitina AO, Apisarov AP, Electrowinning and Annealing of Ir–Re–Ir Material, Tsvetnye Metally, **11** (2017) 55–60. https://doi.org/10.17580/tsm.2017.11.10

16. Ding D, Jin W, Luo W, Ge C, et al., Preparation of Al/TiC Nanocomposite Coatings on 304 Stainless Steel via Electrodeposition in Inorganic Molten Salts, Int. J. Electrochem. Sci., **16** (2021) 21114. https://doi.org/10.20964/2021.11.06

17. Qi W, Ding D, Luo W, Jin W, et al., Production of Al–Mn/WC Composite Coatings with Electrodeposition in $AlCl_3-NaCl-KCl-MnCl_2$ Molten Salts, Coatings, **13** (2023) 1246. https://doi.org/10.3390/coatings13071246

18. Zhang K, Zhu L, Bai S, Ye Y, et al., Ablation Behavior of an Ir-Hf Coating: A Novel Idea for Ultra-High Temperature Coatings in Non-Equilibrium Conditions, J. Alloys Compd., **818** (2020) 152829. https://doi.org/10.1016/j.jallcom.2019.152829

19. Zhu L, Bai S, Zhang H, Ye Y, Gao W, Rhenium Used as an Interlayer between Carbon–Carbon Composites and Iridium Coating: Adhesion and Wettability, Surf. Coat. Technol., **235** (2013) 68–74. https://doi.org/10.1016/j.surfcoat.2013.07.013

20. Gupta SK, Mao Y, Recent Developments on Molten Salt Synthesis of Inorganic Nanomaterials: A Review, The Journal of Physical Chemistry C, **125** (2021) 6508–6533. https://doi.org/10.1021/acs.jpcc.0c10981

21. Gupta SK, Mao Y, A Review on Molten Salt Synthesis of Metal Oxide Nanomaterials: Status, Opportunity, and Challenge, Prog. Mater. Sci., **117** (2021) 100734, https://doi.org/10.1016/j.pmatsci.2020.100734

22. Engelken RD, Ionic Electrodeposition of II–VI and III–V Compounds: IV. Deposition of Both Elements and Compound Positive of the Pure Element Reversible Potentials: Pure Underpotential Deposition, J. Electrochem. Soc., **135** (1988) 834–839. https://doi.org/10.1149/1.2095787

23. Saltykova NA, Portnyagin OV, Electrodeposition of Ir–Ru Alloys from Chloride Melts: Steady-State Potentials and Cathodic Processes, Russian Journal of Electrochemistry, **36** (2000) 784–788. https://doi.org/10.1007/BF02757681

24. Saltykova NA, Portnyagin OV, Electrodeposition of Iridium–Ruthenium Alloys from Chloride Melts: The Structure of the Deposits, Russian Journal of Electrochemistry, **37** (2001) 924–930. https://doi.org/10.1023/A:1011944226271

25. Etenko A, McKechnie T, Shchetkovskiy A, Smirnov A, Oxidation-Protective Iridium and Iridium-Rhodium Coating Produced by Electrodeposition from Molten Salts, ECS Trans., **3** (2007) 151–157. https://doi.org/10.1149/1.2721466

26. Lee Y-J, Lee T-H, Nersisyan HH, Lee K-H, et al., Characterization of Ta–W Alloy Films Deposited by Molten Salt Multi-Anode Reactive Alloy Coating (MARC) Method, Int. J. Refract. Metals Hard Mater., **53** (2015) 23–31. https://doi.org/10.1016/j.ijrmhm.2015.04.022

27. Lee Y-J, Park D-J, Kang K-S, Bae G-G, et al. Molten Salt Multi-Anode Reactive Alloy Coating (Marc) of Ta-W Alloy on Sus316l. In: Proceedings of the 8th Pacific Rim International Congress on Advanced Materials and

Processing; 2013; Springer International Publishing: Cham. pp. 1975–1981. https://doi.org/10.1007/978-3-319-48764-9_245

28. Polyakova LP, Taxil P, Polyakov EG, Electrochemical Behaviour and Codeposition of Titanium and Niobium in Chloride–Fluoride Melts, J. Alloys Compd., **359** (2003) 244–255. https://doi.org/10.1016/S0925-8388(03)00180-4

29. Zhang S, Hu K, Zhao X, Liang J, Li Y, Study on Diffusion Kinetics of Chromium and Nickel Electrochemical Co-Deposition in a NaCl–KCl–NaF–Cr_2O_3–NiO Molten Salt, High Temperature Materials and Processes, **42(1)** (2023) 20220276. https://doi.org/10.1515/htmp-2022-0276

30. Ahmad I, Spiak WA, Janz GJ, Electrodeposition of Tantalum and Tantalum-Chromium Alloys, J. Appl. Electrochem., **11** (1981) 291–297. https://doi.org/10.1007/BF00613946

31. Ueda M, Hayashi H, Ohtsuka T, Electrodeposition of Al–Pt Alloys Using Constant Potential Electrolysis in $AlCl_3$–NaCl–KCl Molten Salt Containing $PtCl_2$, Surf. Coat. Technol., **205** (2011) 4401–4403. https://doi.org/10.1016/j.surfcoat.2011.03.051

32. Sato K, Matsushima H, Ueda M, Electrodeposition of Al-Ta Alloys in NaCl-KCl-$AlCl_3$ Molten Salt Containing $TaCl_5$, Appl. Surf. Sci., **388** (2016) 794–798. https://doi.org/10.1016/j.apsusc.2016.03.001

33. Ueda M, Kigawa H, Ohtsuka T, Co-Deposition of Al–Cr–Ni Alloys Using Constant Potential and Potential Pulse Techniques in $AlCl_3$–NaCl–KCl Molten Salt, Electrochim. Acta, **52** (2007) 2515–2519. https://doi.org/10.1016/j.electacta.2006.09.001

34. Gussone J, Vijay CRY, Watermeyer P, Milicevic J, et al., Electrodeposition of Titanium–Vanadium Alloys from Chloride-Based Molten Salts: Influence of Electrolyte Chemistry and Deposition Potential on Composition, Morphology and Microstructure, J. Appl. Electrochem., **50** (2020) 355–366. https://doi.org/10.1007/s10800-019-01385-0

35. Okamoto H, The Ir-Ru (Iridium-Ruthenium) System, J. Phase Equilib., **13** (1992) 565–567. https://doi.org/10.1007/BF02665768

36. Chamelot P, Palau P, Massot L, Savall A, Taxil P, Electrodeposition Processes of Tantalum(V) Species in Molten Fluorides Containing Oxide Ions, Electrochim. Acta, **47** (2002) 3423–3429. https://doi.org/10.1016/S0013-4686(02)00278-5

37. Smith JF, The Deposition of Chromium from a Fused Fluoride Electrolyte, Thin Solid Films, **95** (1982) 151–160. https://doi.org/10.1016/0040-6090(82)90237-1

38. Turchi PEA, Abrikosov IA, Burton B, Fries SG, et al., Interface between Quantum-Mechanical-Based Approaches, Experiments, and CALPHAD Methodology, Calphad, **31** (2007) 4–27. https://doi.org/10.1016/j.calphad.2006.02.009

39. Ankem S, Margolin H, Greene C, Neuberger B, Oberson P, Mechanical Properties of Alloys Consisting of Two Ductile Phases, Prog. Mater. Sci., **51** (2006) 632–709. https://doi.org/10.1016/j.pmatsci.2005.10.003

40. Cochrane RW, Harris R, Zuckermann MJ, The Role of Structure in the Magnetic Properties of Amorphous Alloys, Phys. Rep., **48** (1978) 1–63. https://doi.org/10.1016/0370-1573(78)90012-1

41. Whang SH. Nanostructured Metals and Alloys: Processing, Microstructure, Mechanical Properties and Applications. Elsevier: Amsterdam, The Netherlands; 2011. 840 p.

42. Schoenitz M, Dreizin EL, Structure and Properties of Al–Mg Mechanical Alloys, J. Mater. Res., **18** (2003) 1827–1836. https://doi.org/10.1557/JMR.2003.0255

43. Vinogradov-Zhabrov ON, Minchenko LM, Esina NO, Pankratov AA, Electrodeposition of Rhenium from Chloride Melts: Electrochemical Nature, Structure and Applied Aspects, Journal of Mining and Metallurgy, Section B: Metallurgy, **39** (2003) 149–166. https://doi.org/10.2298/JMMB0302149V

44. Li F, Zhu L, Zhang K, Wang Z, et al., Oxidation Behaviors of Ir-Hf and Ir-Zr Coatings under Different Air Pressures at 1800 °C, Surf. Coat. Technol., **466** (2023) 129640. https://doi.org/10.1016/j.surfcoat.2023.129640

45. Zhang K, Zhu L, Bai S, Ye Y, et al., Ablation Behavior of an Ir-Hf Coating: A Novel Idea for Ultra-High Temperature Coatings in Non-Equilibrium Conditions, J. Alloys Compd., **818** (2020) 152829. https://doi.org/10.1016/j.jallcom.2019.152829

46. Yang L, Jing L, Zhang J, Liu L, et al., New Insights on the Ablation Mechanism of Silicon Carbide in Dissociated Air Plasmas, Aerosp. Sci. Technol., **129** (2022) 107863. https://doi.org/10.1016/j.ast.2022.107863

47. Cui E, Wang C, Zuo Y, Leng B, et al., Preparation of Iridium-hafnium Intermetallic Compound Coatings in Molten Salts, Surf. Coat. Technol., **427** (2021) 127821. https://doi.org/10.1016/j.surfcoat.2021.127821